



## **FRET with MoS2 nanosheets integrated CRISPR/Cas12a sensors for robust and visual food-borne parasites detection**

Xiuqin Chen, Xiaolei Liu, Yao Yu, Haolu Wang, Chengyao Li, Isabelle Vallée,  
Mingyuan Liu, Lianjing Zhao, Xue Bai

### **► To cite this version:**

Xiuqin Chen, Xiaolei Liu, Yao Yu, Haolu Wang, Chengyao Li, et al.. FRET with MoS2 nanosheets integrated CRISPR/Cas12a sensors for robust and visual food-borne parasites detection. Sensors and Actuators B: Chemical, 2023, 395, pp.134493. 10.1016/j.snb.2023.134493 . anses-04369914

**HAL Id: anses-04369914**

**<https://anses.hal.science/anses-04369914>**

Submitted on 9 Apr 2024

**HAL** is a multi-disciplinary open access archive for the deposit and dissemination of scientific research documents, whether they are published or not. The documents may come from teaching and research institutions in France or abroad, or from public or private research centers.

L'archive ouverte pluridisciplinaire **HAL**, est destinée au dépôt et à la diffusion de documents scientifiques de niveau recherche, publiés ou non, émanant des établissements d'enseignement et de recherche français ou étrangers, des laboratoires publics ou privés.



# FRET with MoS<sub>2</sub> nanosheets integrated CRISPR/Cas12a sensors for robust and visual food-borne parasites detection

Xiuqin Chen<sup>a,b,1</sup>, Xiaolei Liu<sup>a,1</sup>, Yao Yu<sup>a</sup>, Haolu Wang<sup>a</sup>, Chengyao Li<sup>a</sup>, Isabelle Vallée<sup>c</sup>, Mingyuan Liu<sup>a,d,\*</sup>, Lianjing Zhao<sup>a,\*\*</sup>, Xue Bai<sup>a,\*\*</sup>

<sup>a</sup> State Key Laboratory for Diagnosis and Treatment of Severe Zoonotic Infectious Diseases, Key Laboratory for Zoonosis Research of the Ministry of Education, Institute of Zoonosis, and College of Veterinary Medicine, Jilin University, Changchun 130062, China

<sup>b</sup> Institute of Animal Husbandry and Veterinary Medicine, Fujian Academy of Agricultural Science, Fuzhou 350013, China

<sup>c</sup> ANSES, École Nationale Vétérinaire d'Alfort, INRAE, UMR BIPAR, Laboratoire Santé Animale, Maisons-Alfort 97400, France

<sup>d</sup> Jiangsu Co-innovation Center for Prevention and Control of Important Animal Infectious Diseases and Zoonoses, Yangzhou 225000, China

## ARTICLE INFO

### Keywords:

CRISPR/Cas12a  
MoS<sub>2</sub> nanosheets  
Förster resonance energy transfer  
Point-of-care testing  
Parasite detection

## ABSTRACT

Recently, CRISPR/Cas associated biosensors have been shown to have great potential in sensing applications due to their high sensitivity and high base resolution. However, the signal reporter system containing two organic fluorescent dye pair is limited by high cost and less stability. In contrast, functional nanomaterials exhibit robust stability, excellent optical properties and low preparation cost, making them suitable reporters. In this study, a MoS<sub>2</sub> nanosheets (NSs) improved CRISPR/Cas12a-based biosensing platform was constructed for the first time to detect food-borne parasites. MoS<sub>2</sub> NSs were used as fluorescence quenchers and single-stranded DNA (ssDNA) discriminated carrier to construct CRISPR/Cas signal reporter system. The combination of recombinase polymerase amplification with MoS<sub>2</sub> NSs modulated CRISPR/Cas12a helped achieve attomolar sensitivity for nucleic acid detection within 35 min. Moreover, the results were obtained using a portable apparatus, enabling visual detection at the point of care. The practical applicability of this biosensing platform was successfully achieved through the detection of anisakis in real samples. This study provides novel insights into exploring the feasibility of two-dimensional nanomaterials based reporter in the CRISPR/Cas12a system, as well as offers a reliable tool for on-site monitoring of parasites.

## 1. Introduction

Food-borne parasitic diseases (FBPDs) have emerged as a global public health concern. Subsequently, rapid and accurate diagnosis of food-borne parasites is crucial to prevent FBPDs. The detection of nucleic-acid is an accurate molecular diagnostics method frequently leveraged for FBPDs diagnosis. Although the polymerase chain reaction (PCR) is a gold-standard technique for nucleic-acid diagnostics, its application in point-of-care (POC) diagnosis is significantly limited by its requirement of sophisticated analytical instruments and long turn-around time (>2 h) [1,2]. Over the last few decades, biosensors have been extensively applied for disease diagnosis, food safety, and environmental monitoring [3]. Of them, fluorescence-based optical

biosensors are most widely used due to their effectiveness, operation convenience and recent advancements in novel dyes and fluorescent probes [4]. The optical biosensors based on Förster resonance energy transfer (FRET) sensing strategy have the advantages of fast response, excellent sensitivity, selectivity and wash-free detection of targets [5]. The FRET is mainly based on energy transfer from an excited state donor to a ground state acceptor in a distance-dependent manner [5,6]. One of the premises of FRET is that the emission spectrum of the donor overlaps with the absorption spectrum of the acceptor [6]. Based on the above theory, various FRET-based biosensors have been fabricated to detect nucleic acids, antibodies, enzymes, small molecules and compounds [6]. Nevertheless, the conventional FRET-based strategy has several limitations, such as a short fluorescence lifetime of organic dye and cross-talk

\* Corresponding author at: State Key Laboratory for Diagnosis and Treatment of Severe Zoonotic Infectious Diseases, Key Laboratory for Zoonosis Research of the Ministry of Education, Institute of Zoonosis, and College of Veterinary Medicine, Jilin University, Changchun 130062, China.

\*\* Corresponding authors.

E-mail addresses: [liumy36@163.com](mailto:liumy36@163.com) (M. Liu), [lianjingzhao@jlu.edu.cn](mailto:lianjingzhao@jlu.edu.cn) (L. Zhao), [namiya23@163.com](mailto:namiya23@163.com) (X. Bai).

<sup>1</sup> These authors contributed equally to this work.

**Table 1**

Nucleic acids sequences employed in this study.

Name	*Sequence (5'-3')
5 nt reporter	FAM- <b>TTATT</b>
10 nt reporter	FAM- <b>TTTTTTTATT</b>
15 nt reporter	FAM- <b>TTTTTTTTTTTTTATT</b>
20 nt reporter	FAM- <b>TTTTTTTTTTTTTTTTTTTATT</b>
30 nt reporter	FAM- <b>TTTTTTTTTTTTTTTTTTTTTTTTTTTATT</b>
FQ reporter	FAM- <b>TTATT</b> -BHQ
gRNA1	UAAUUUCUACUAAGUGUAGAU <b>AUAGGGGCAACAACCAGCAUAC</b>
gRNA2	UAAUUUCUACUAAGUGUAGAU <b>AUAGGGGCAACAACCAGCAU</b>
gRNA3	UAAUUUCUACUAAGUGUAGAU <b>GUGGUCACAAAAGUGACAAG</b>
gRNA4	UAAUUUCUACUAAGUGUAGAU <b>UCAUCACUAAGCAAGGAACCG</b>

\* The difference of five FAM-labeled reporters is labeled in blue. The spacer sequences of the gRNAs, which recognize and complement the target, are labeled in red color. FAM: carboxyfluorescein; BHQ: Black Hole Quencher®.

issue [7,8].

With the development of material science, nanomaterials involved in FRET have been widely applied for biological analysis. For instance, MoS<sub>2</sub> nanosheets (NSs) [9–11], graphene oxide [12–14] and gold nanoparticles [15–17] have been used to fabricate FRET-based detection strategies due to their benefits of prolonged fluorescence lifetime, tunable emission, and wide absorption spectrum [7]. Of them, MoS<sub>2</sub> NSs, a two-dimensional (2D) nanomaterial analogous to graphene, are the most promising due to their unique and appealing properties. Firstly, MoS<sub>2</sub> NSs can be easily functionalized with biomolecules [18]. Secondly, MoS<sub>2</sub> NSs exhibit high absorption capability and different affinities toward single-stranded DNA (ssDNA) and double-stranded DNA (dsDNA) [9,19,20]. Furthermore, MoS<sub>2</sub> NSs exhibit stronger fluorescence quenching capability than common organic fluorescence quenched molecules [20]. Therefore, the ssDNA-labeled fluorophore may form an excellent donor-acceptor pair with MoS<sub>2</sub> NSs. Based on the above theory, Zhang et al. [9] constructed a FRET-based fluorescent DNA biosensor for the first time. And the sensitivity of the FRET-based nanobiosensors could be greatly improved with the aid of isothermal amplification techniques, such as recombinase polymerase amplification (RPA) and loop-mediated isothermal amplification (LAMP) [21,22]. Unfortunately, the disadvantages of non-specific amplification and complicated primers design greatly limit their further applications [21, 23]. Consequently, these problems are driving innovations of novel signal transduction patterns for nucleic acid detection.

Recently, the clustered regularly interspaced short palindromic repeats (CRISPR) and CRISPR-associated (Cas) proteins system has attracted increasing attention due to the discovery of trans-cleavage activity of some Cas proteins [24–26]. Among the accessible Cas family members, Cas12a protein (also known as Cpf1) has been proven to be a promising candidate for nucleic acid detection. With the aid of guide RNA (gRNA), the Cas12a protein can specifically recognize and capture

the dsDNA target with a T nucleotide-rich protospacer adjacent motif (PAM) sequence. Then the RuvC catalytic domain of Cas12a protein is triggered to indiscriminately digest the surrounding ssDNA (at a rate of thousands of turnovers per second), resulting in the separation of the fluorophore and quenching molecule, thereby achieving the goal of signal amplification [24]. Based on this phenomenon, the target nucleic acid information can be converted into electrochemical [27,28], colorimetric [29,30], fluorescent [31,32] and bioluminescent readout [33, 34]. Moreover, the CRISPR/Cas12a system poses significant characteristics, such as recognition at a mild reaction temperature, flexibility of the design and prominent signal amplification efficiency capability, serving as a powerful toolbox in molecular diagnosis [35]. Despite tremendous achievements, the current CRISPR/Cas12a-based biosensors commonly use organic dyes as fluorophores and quenchers at both ends of ssDNA for signal output, which is not cost-effective and requires an elaborate choice of fluorescence donor-acceptor pairings to form FRET [36]. Furthermore, they might result in a high fluorescence background, limiting the overall sensitivity [37]. Metal nanoclusters as a class of novel fluorophores, have been applied for fabricating CRISPR/Cas-mediated biosensors due to their appealing characteristics, such as good biocompatible, photostability and simple to synthesis [36, 38,39]. However, it is still difficult to precisely control the size of metal nanoclusters with high yields [40]. Moreover, the problems of low quantum yield and poor stability further limit their application [41]. Therefore, designing a simple and economical probe to be applied in the CRISPR/Cas-based biosensing platform is of great significance.

In this study, a universal CRISPR/Cas12a-modulated FRET-based biosensing platform was constructed for nucleic acids detection using MoS<sub>2</sub> NSs as fluorescence quenchers and ssDNA discriminated carrier. This detection strategy was realized by taking advantage of the excellent quenching ability of MoS<sub>2</sub> NSs and the variability of the adsorption capability of MoS<sub>2</sub> NSs toward different probes lengths. In the absence of

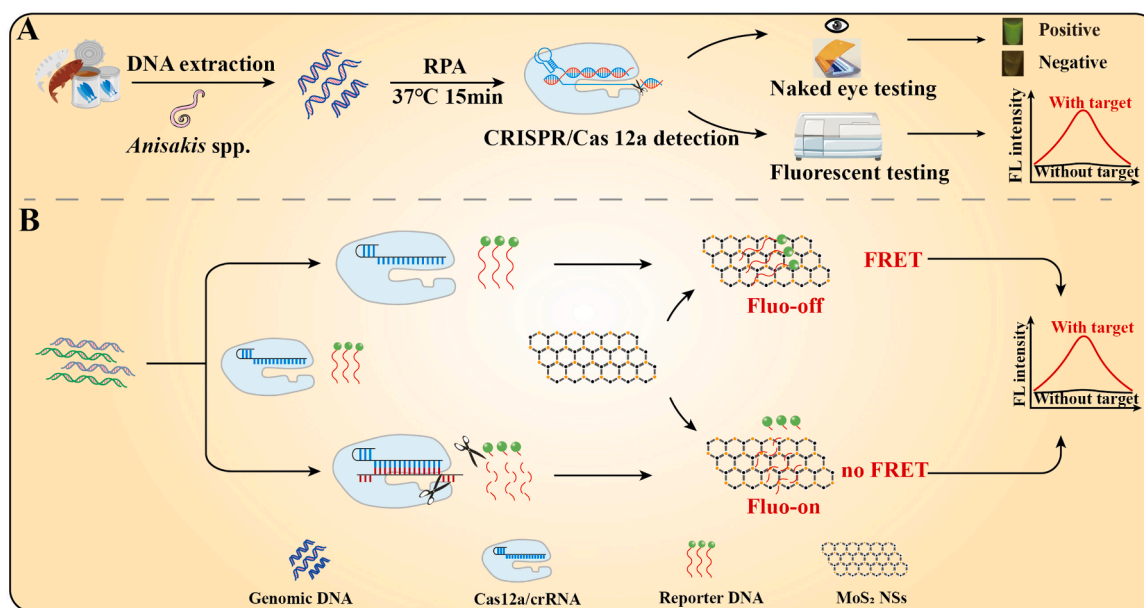


Fig. 1. Schematics illustration of the principle of MoS<sub>2</sub> NSs-CRISPR/Cas12a biosensing platform for detecting nucleic acid.

the target DNA, the fluorescence of ssDNA-FAM was quenched by MoS<sub>2</sub> NSs due to the FRET effect, and the biosensor was on a “turn-off” status. In the presence of the target DNA, a ternary complex of Cas12a, gRNA, and dsDNA exhibiting cleavage activity was formed. Afterwards, the ssDNA-FAM reporter was cleaved into short fragments by the activated Cas12a, facilitating the detachment of the fluorophore FAM labeled on ssDNA from the surface of MoS<sub>2</sub> NSs and the restoration of the fluorescence signal. Therefore, a novel “turn-on-off” biosensing platform was fabricated for nucleic acids detection. Notably, visible results were observed without any sophisticated equipment, which was friendly to low resource areas and suitable for POC diagnosis application. Overall, the experimental results provide novel insights into the fabrication of a universal DNA biosensing platform based on 2D nanomaterials combined with CRISPR/Cas systems.

## 2. Experimental section

### 2.1. Materials and apparatus

LbCas12a protein, NEBuffer 2.1 (10×) and NEBuffer 3.1 (10 ×) were obtained from New England Biolabs (Beijing, China). 10× reaction buffer was supplied by Guangzhou Magigen Biotechnology Co., Ltd. (Guangzhou, China). Molybdenum disulfide (MoS<sub>2</sub>) nanosheets were purchased from Nanjing XF Nano Material Tech Co., Ltd. (Nanjing, China), and the stock concentration was 1.0 mg/mL. Dithiothreitol (DTT) was purchased from Solarbio Science & Technology Co., Ltd. (Beijing, China). An RPA assay kit was purchased from TwistDx Ltd. (Cambridge, UK). A TIANamp genomic DNA kit was purchased from Tiangen Biotech (Beijing, China). Premix Ex Taq Probe qPCR was provided by TaKaRa Biotechnology Co., Ltd (Dalian, China). The gRNAs for specifically recognizing the sequences were designed through the Benchling Web site (<https://www.benchling.com/crispr/>).

All the DNA oligonucleotide sequences were synthesized in Sangon Biotech (Shanghai, China). The nucleotide sequences are listed in Table 1.

A transmission electron microscope (JEOL TEM-3010, Japan) was used to observe the morphology of MoS<sub>2</sub> NSs. A multi-mode microplate reader (CYTATION 5, BioTek, USA) was utilized to obtain the fluorescence spectra and UV–vis absorbance. A Mastercycler ep realplex system (Eppendorf, Germany) was used for TaqMan qPCR assay.

### 2.2. RPA reaction assay

The RPA assay was performed according to the instructions with slight modifications (refer to the [Supporting Information](#) for RPA assay). The primers sequences are listed in Table S1.

### 2.3. Detection of nucleic acid with the MoS<sub>2</sub> NSs-CRISPR/Cas12a nanoplatform

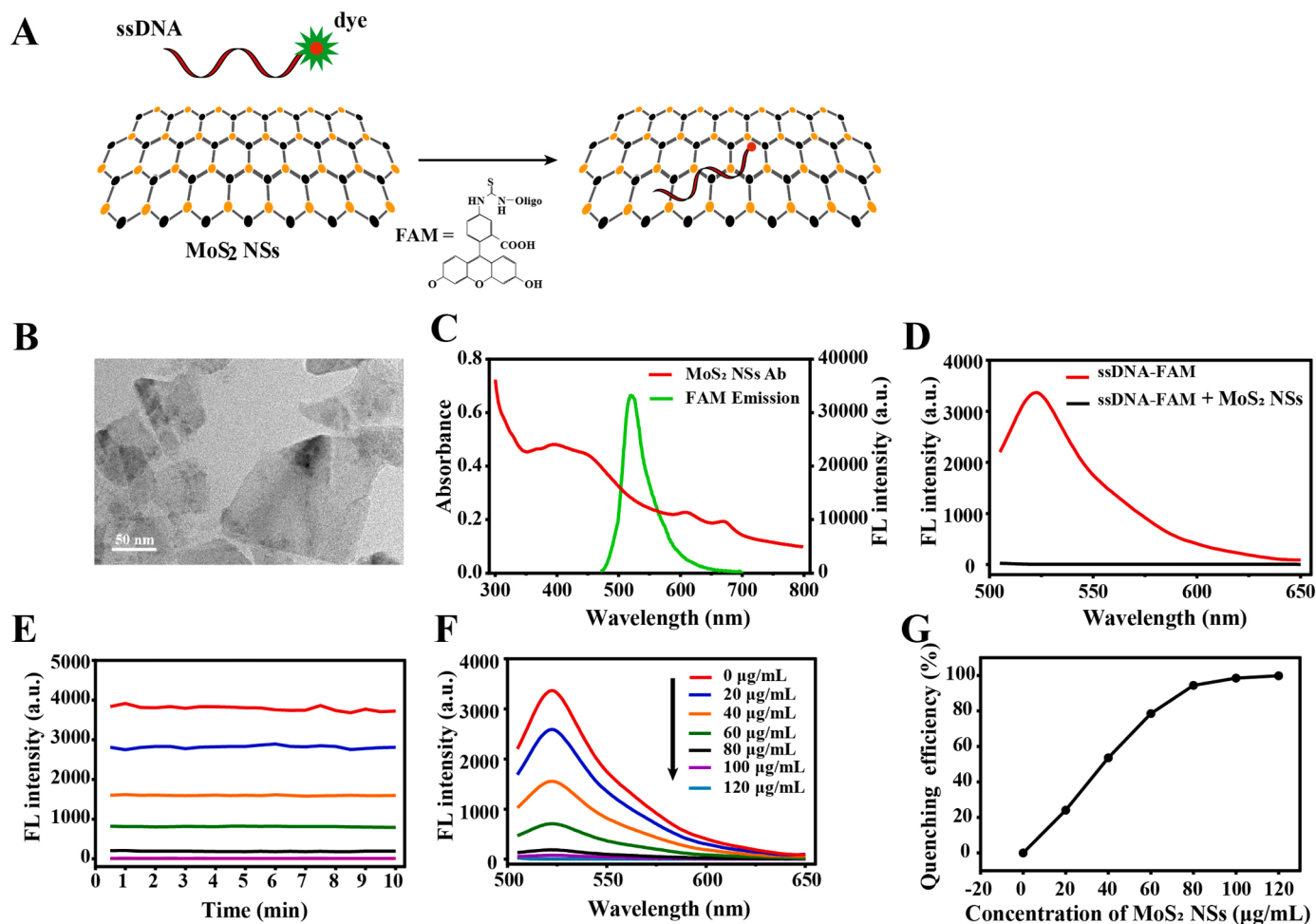
The assay was performed in a 30 µL reaction solution. Firstly, 50 nM of Cas12a was preincubated with 100 nM gRNA in 10× Magigen reaction buffer (the components are listed in Table S2) at 37 °C for 10 min. Subsequently, 100 nM of ssDNA-FAM reporter and 3 µL of RPA amplicons were added, followed by incubation at 37 °C for 10 min. Afterwards, a certain amount of MoS<sub>2</sub> NSs was added to the trans-cleavage reaction. Finally, the fluorescence spectra were recorded immediately using a fluorescence microplate reader.

### 2.4. Sensitivity and selectivity of the MoS<sub>2</sub> NSs-CRISPR/Cas12a nanoplatform

1 µL of tenfold serial dilutions of plasmid DNA (10<sup>5</sup> – 10<sup>1</sup> aM) was used as the template for amplification by RPA. Then, 3 µL of RPA amplicons were used for activating the Cas12a cleaving system. As for selectivity evaluation, three different fish-borne parasites (including *Hysterothylacium aduncum*, *Clonorchis sinensis* and *Ligula intestinalis*) and one marine fish tissue (*Trichirurus lepturus*) was used.

### 2.5. Validation of the MoS<sub>2</sub> NSs-CRISPR/Cas12a nanoplatform for *Anisakis* spp. detection with spiked samples

*Trichirurus lepturus* samples and fish-derived food samples were purchased from local supermarkets. The absence of anisakids in samples was confirmed using qPCR [42]. The spiked samples were analyzed according to the previously reported method with slight modification (refer to **Artificially contaminated fish samples** in [Supporting Information](#) [42]). A blue light gel imager was used for visual detection to facilitate POC detection (**Visual detection**, [Supporting Information](#)).



**Fig. 2.** The fluorescence quenching ability of MoS<sub>2</sub> NSs. (A) Schematic illustration of fluorescence quenching of MoS<sub>2</sub> NSs. (B) Transmission electron microscopy image of MoS<sub>2</sub> NSs. (C) UV–vis absorbance of MoS<sub>2</sub> NSs and the fluorescence emission spectra of FAM dye. (D) Fluorescence spectra obtained before (red curve) and after (black curve) the addition of MoS<sub>2</sub> NSs. Real-time fluorescence curves (E) and Fluorescence spectra (F) of ssDNA-FAM under different concentrations of MoS<sub>2</sub> NSs. The final concentration of ssDNA-FAM was 100 nM. MoS<sub>2</sub> NSs concentration range: 0–120 µg/mL. (G) The fluorescence quenching efficiency of MoS<sub>2</sub> NSs under different MoS<sub>2</sub> NSs concentrations. The fluorescence quenching efficiency was calculated as follows:  $QE = (F_0 - F)/F_0 \times 100\%$ , where  $F_0$  and  $F$  are the fluorescence intensity without and with the addition of MoS<sub>2</sub> NSs ( $\lambda_{ex}$  485 nm,  $\lambda_{em}$  525 nm).

### 3. Results and discussion

#### 3.1. Mechanism of MoS<sub>2</sub> NSs-CRISPR/Cas12a nanoplatform

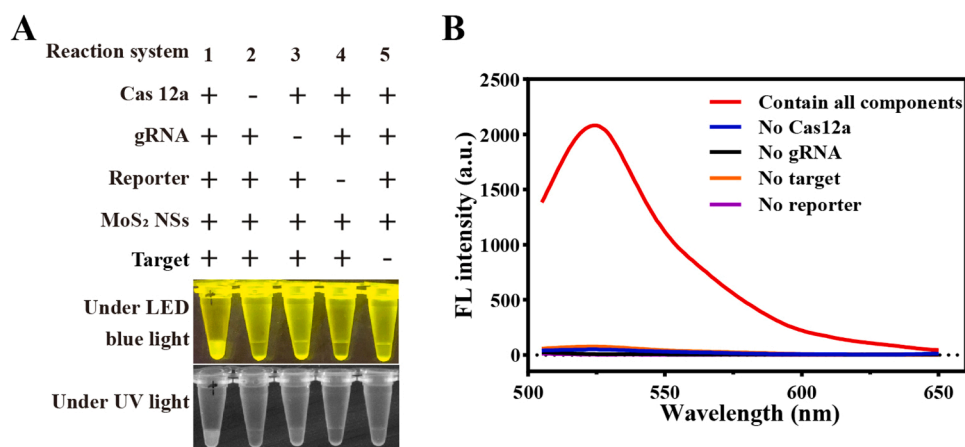
The biosensing platform for nucleic acid detection can be divided into two processes involving target DNA isothermal amplification and MoS<sub>2</sub> NSs-CRISPR/Cas12a detection (Fig. 1). Firstly, the genomic DNA of different samples were extracted using a commercial kit. Then the genomic DNA was added to the RPA system at 37 °C for 15 min to amplify the target nucleic acid. Later, the amplicons were subjected to CRISPR/Cas12a trans-cleavage reaction at 37 °C. The fluorescent signal was read out using a blue light gel imager or a fluorescence detector within 20 min (Fig. 1A). As for the MoS<sub>2</sub> NSs-CRISPR/Cas12a detection principle, the Cas12a trans-cleavage activity was silenced in the absence of target DNA and appropriate length of FAM-labeled ssDNA (ssDNA-FAM) reporters were adsorbed on the surface of MoS<sub>2</sub> NSs in a close proximity through van der Waals force [43]. Then, the FRET between the fluorophore and MoS<sub>2</sub> NSs was triggered, resulting in quenching of the fluorescence of FAM by MoS<sub>2</sub> NS (Fig. 1B). While in the presence of the target DNA, the Cas12a protein combined with the target DNA and specific gRNA to form a ternary complex. Afterwards, the indiscriminate cleavage activity of Cas12a was triggered to shear the ssDNA-FAM reporters into short fragments. Consequently, the fluorophore FAM

labeled on ssDNA dissociated from the MoS<sub>2</sub> NSs surface due to the weakening of the adsorption force. Thus, the FRET effect between ssDNA-FAM and MoS<sub>2</sub> NSs was hindered, resulting in the recovery of the fluorescence signal (Fig. 1B). Meanwhile, a second signal amplification was achieved in the CRISPR/Cas12a system. The intensity of the fluorescence output signal was correlated with the concentration of the activated Cas12a/gRNA, which relied on the concentration of the target DNA. Therefore, the presence and concentration of target DNA can be determined by monitoring the change in the fluorescence intensity of the reaction. Moreover, the proposed detection strategy can be transformed into a universal biosensing platform by programming the gRNA sequence to detect any nucleic-acid targets.

#### 3.2. Feasibility verification of the proposed biosensing platform

The microstructure of MoS<sub>2</sub> NSs, i.e., the size and morphology, were characterized using transmission electron microscopy. As shown in Fig. 2B, the MoS<sub>2</sub> NSs exhibited a sheet structure, providing a large surface area for adsorption. The diameter of MoS<sub>2</sub> NSs was in the range of several nanometers to hundreds of nanometers. The UV–vis optical absorption measurement results revealed that the MoS<sub>2</sub> NSs had a wide absorption spectral range from 300 to 800 nm, and two characteristic absorption peaks of MoS<sub>2</sub> NSs were located at about 600–700 nm





**Fig. 3.** Feasibility validation of the MoS<sub>2</sub> NSs-CRISPR/Cas12a assay. (A) Visual readouts of five reaction systems with various components through endpoint imaging. The images were captured under blue light (470 nm) and the gel imaging system using UV light after being incubated for 10 min. (B) Spectrogram fluorescence of CRISPR/Cas12a-mediated ssDNA-FAM reporter cleavage. Except for the red curve, the others refer to the reaction without the corresponding single component but contained all other components and enzymes ( $\lambda_{ex}$  485 nm,  $\lambda_{em}$  525 nm). A 15 nt ssDNA-FAM reporter was used. The concentrations of Cas12a, gRNA, ssDNA-FAM reporter and MoS<sub>2</sub> NSs were 50 nM, 100 nM, 100 nM, and 100  $\mu$ g/mL, respectively.

(Fig. 2C). The overlap of the absorption spectrum of MoS<sub>2</sub> NSs with the fluorescence emission of FAM dye made it feasible to construct an efficient FRET-based biosensor (Fig. 2C).

Unlike a double labeled DNA reporter used in most previous studies [24,32,44], ssDNA-FAM reporters and MoS<sub>2</sub> NSs were employed in this study to fabricate FRET-based biosensor using fluorophore (FAM) as a FRET donor and MoS<sub>2</sub> NSs as FRET acceptors. As shown in Fig. 2A, the ssDNA-FAM reporters were adsorbed on the surface of MoS<sub>2</sub> NSs through the van der Waals force [43]. Then, the FRET between the fluorophore and MoS<sub>2</sub> NSs was activated, resulting in the quenching of the fluorescence of FAM by MoS<sub>2</sub> NSs. The fluorescence spectra with or without MoS<sub>2</sub> NSs were recorded to validate the quenching capability of MoS<sub>2</sub> NSs. As shown in Fig. 2D, the ssDNA-FAM exhibited a strong fluorescence signal at 525 nm wavelength in the absence of MoS<sub>2</sub> NSs (red curve). However, when MoS<sub>2</sub> NSs (final concentration was 100  $\mu$ g/mL) were added to the above mixture, the fluorescence signal was almost completely quenched (black curve), exhibiting super fluorescence quenching ability. These results demonstrated the MoS<sub>2</sub> NSs could serve as a good fluorescent quencher towards FAM dye. Later, the ratio of ssDNA-FAM and MoS<sub>2</sub> NSs was optimized to achieve high quenching efficiency. Thus, ssDNA-FAM with fixed concentration (1  $\mu$ M) was incubated with a series of concentrations of MoS<sub>2</sub> NSs ranging from 0 to 120  $\mu$ g/mL in 10  $\times$  Magigen reaction buffer. As shown in Fig. 2E and F, the fluorescence intensity at 525 nm gradually decreased with increased MoS<sub>2</sub> NSs concentration. Moreover, the fluorescence quenching was extremely fast and about 98.5 % of fluorescence was rapidly quenched within 5 min (Fig. 2E). When the concentration of MoS<sub>2</sub> NSs was 100  $\mu$ g/mL, the fluorescence quenching efficiency almost reached a plateau (Fig. 2G). Therefore, the concentration of MoS<sub>2</sub> NSs was maintained at 100  $\mu$ g/mL for the following MoS<sub>2</sub> NSs-CRISPR/Cas12a assay. Additionally, the effect of reaction temperature on the quenching ability of MoS<sub>2</sub> NSs was investigated. The best quenching efficiency of MoS<sub>2</sub> NSs was observed below 37  $^{\circ}$ C (Fig. S1). Considering the temperatures at which Cas12a exerted the best activity, and RPA achieved the best amplification efficiency, the reaction temperature of the proposed assay was set at 37  $^{\circ}$ C.

Five reaction systems (reactions # 1–5) with various components were prepared and tested to systematically evaluate the feasibility of the proposed assay (Fig. 3A). A plasmid containing 192 bp of *Anisakis* spp. internal transcribed spacer sequence fragment was used as the target (Fig. S2). After incubation at 37  $^{\circ}$ C for 10 min, only reaction # 1 containing all components generated a bright fluorescence signal under LED blue light or UV light. While the absence of arbitrary components in the detection systems made the assay invalid (Fig. 3A). The fluorescent intensity measurement results validated the visual readout further (Fig. 3B). These results revealed that the CRISPR/Cas12a system is compatible with the MoS<sub>2</sub> NSs-ssDNA FRET-based system, and the

collateral cleavage activity of Cas12a performed well in the fabricated MoS<sub>2</sub> NSs-CRISPR/Cas12a biosensing platform.

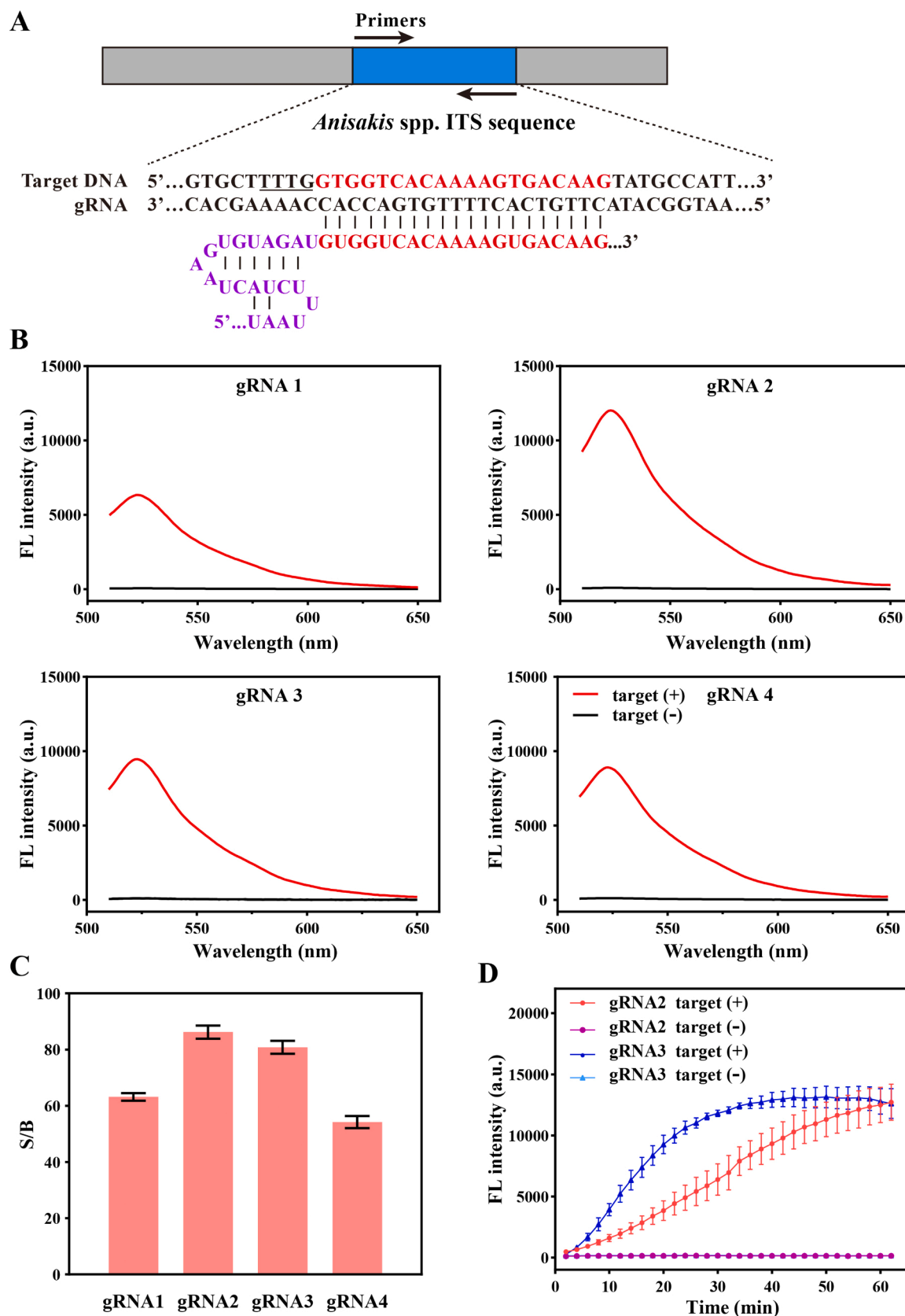
### 3.3. Optimization of the biosensing conditions

Several vital experiment conditions were optimized, including the gRNA sequence, fluorescence quenching strategy, the ratio of Cas12a to gRNA, the length of ssDNA reporters and buffers to achieve excellent analytical performance for nucleic acids detection. Firstly, the gRNA sequence was optimized. As shown in Fig. 4B, gRNA2 and gRNA3 achieved significantly higher fluorescence intensity than those of the other two gRNAs. The same result was found for the signal-to-background ratio (S/B) of four gRNAs (Fig. 4C). The low S/B ratio might be contributed to the complex secondary structure of the gene, making the gRNA hard to bind [45]. As shown in Fig. 4D, the fluorescence intensity of gRNA3 increased faster than gRNA2, indicating that gRNA3 had a better activation efficiency than Cas12a. Therefore, gRNA3 was selected for subsequent experiments. The gRNA3 sequence (20 nt) is shown in Fig. 4A.

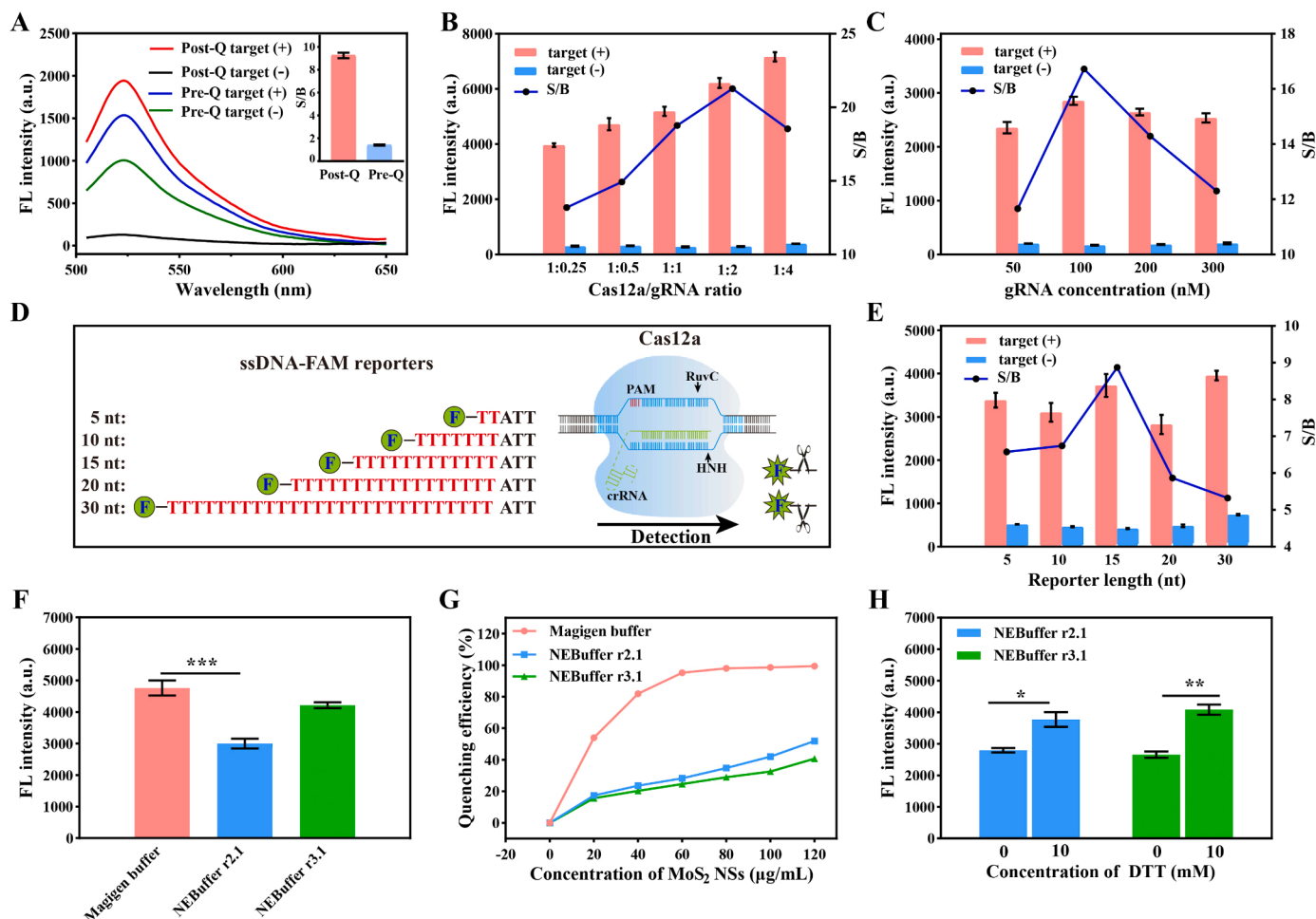
Later, the effect of pre-quenching and post-quenching strategy on the trans-cleavage efficiency of Cas12a was explored by changing the adding order of ssDNA-FAM reporter and MoS<sub>2</sub> NSs. The post-quenching strategy was performed as described in the methods. As for the pre-quenching strategy, the ssDNA-FAM reporter was mixed with MoS<sub>2</sub> NSs and then the mixture was added to the CRISPR/Cas12a system. As shown in Fig. 5A, the S/B of the pre-quenching strategy was significantly lower than the post-quenching strategy. For the pre-quenching strategy, the adsorption of ssDNA probes on the surface of MoS<sub>2</sub> NSs forms steric hindrance, resulting in a decrease in the efficiency of ssDNA cleavage by Cas12a. Therefore, the post-quenching strategy was performed for the following experiments.

In the CRISPR/Cas system, the amount of Cas/gRNA complex determines the speed of the shearing reaction, and the concentration ratio of the Cas enzyme to gRNA is critical to obtain an optimal signal readout [44]. Therefore, various concentration ratios of Cas12a to gRNA were investigated. As depicted in Fig. 5B, the S/B ratio reached the maximum when the ratio of Cas12a to gRNA was 1:2. It is reported that a proper excess amount of gRNA is beneficial for the Cas12a ternary complex formation [46]. As for the concentration of gRNA, the maximum S/B ratio was achieved when the gRNA concentration was 100 nM (Fig. 5C). Therefore, the optimized concentrations of Cas12a and gRNA were chosen at 50 nM and 100 nM, respectively.

Further, the length of the ssDNA could determine the sensitivity of the established biosensing platform by affecting the length of the fragments cut by CRISPR/Cas12a and the interaction between the ssDNA reporter and MoS<sub>2</sub> NSs. Therefore, the length of the ssDNA reporter should be optimized further. Five reporters of different base lengths



**Fig. 4.** Screening of the candidate gRNAs for detecting *Anisakis* spp. nucleic acid. (A) Design of the gRNA sequence based on the ITS sequence of *Anisakis* spp. The fluorescence spectra (B) and signal-to-background ratio (S/B) (C) of MoS<sub>2</sub> NSs-CRISPR/Cas12a assay for detecting *Anisakis* spp. nucleic acid using four different gRNAs. (D) Real-time fluorescence curves of the assay using gRNA2 and gRNA3. Error bars represent standard deviation obtained from three parallel experiments.



**Fig. 5.** Optimization of the experimental conditions. (A) Effect of adding order of the ssDNA-FAM reporter and MoS<sub>2</sub> NSs on the trans-cleavage efficiency. Inset: S/B ratio of two different quenching strategies. Post-Q and Pre-Q stand for post-quenching strategy and pre-quenching strategy, respectively. (B) Molar ratio optimization of Cas12a/gRNA. (C) Optimization of gRNA concentration. (D) Schematic diagram of various lengths of reporters labeled with FAM and subjected to Cas12a reaction. (E) Fluorescence response of different lengths of ssDNA reporter. (F) The effect of different buffers on trans-cleavage efficiency of CRISPR/Cas12a. (G) The effect of different buffers on quenching efficiency of MoS<sub>2</sub> NSs. (H) The trans-cleavage efficiency of CRISPR/Cas12a in two different buffers by supplement with DTT. The final concentration of DTT in buffers was 10 mM. Error bars represent the mean  $\pm$  standard deviation (SD), of three experimental replicates. \*,  $P < 0.05$ , \*\*,  $P < 0.01$ , \*\*\*,  $P < 0.001$ . The unpaired two-tailed t-test was used to analyze the statistical significance.

were designed (Fig. 5D). As presented in Fig. 5E, the length of the 15 nt reporter achieved the highest S/B. Nonetheless, if the length of the ssDNA reporter is too short or too long, output fluorescence signal decreases. This might be attributed to the fact that the length of the ssDNA reporter affects the adsorption between ssDNA and MoS<sub>2</sub> NSs and thus further affects FRET. The second reason could be that the length of the ssDNA reporter determines the signal amplification efficiency. For the same collateral cleavage activity of Cas12a, a longer ssDNA reporter might produce a less fluorescent signal upon shearing. A similar result was observed for the effect of different lengths of ssDNA-FAM reporter on the quenching ability of MoS<sub>2</sub> NSs (Fig. S3). The different adsorption capacities of MoS<sub>2</sub> NSs toward different lengths of ssDNA revealed that MoS<sub>2</sub> NSs can be used as a discriminated carrier of ssDNA. Therefore, a length of 15 nt reporter was selected for further application.

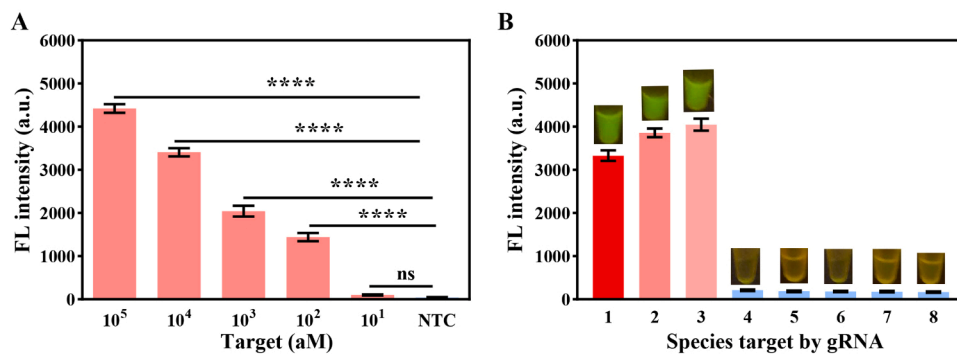
Finally, the spontaneous formation of a higher-level structure essential for protein function is mainly determined by the buffer components, which might affect the trans-cleavage efficiency of Cas12a [47]. Moreover, some chemicals could affect the adsorption and desorption of MoS<sub>2</sub> NSs [48]. Therefore, the trans-cleavage efficiency of the Cas12a system and the quenching efficiency of MoS<sub>2</sub> NSs were investigated in three commercial CRISPR/Cas buffers. As shown in Fig. 5F, Cas12a in the Magigen buffer exhibited the best trans-cleavage

efficiency. A similar result was found for the quenching efficiency of MoS<sub>2</sub> NSs (Fig. 5G). Compared to the other two buffers, only the Magigen buffer contained DTT (Table S2). DTT is widely used to stabilize enzyme by preventing the formation of disulfide bonds in proteins [49,50]. Therefore, it was speculated that DTT might play a major role in enhancing the collateral cleavage efficiency of CRISPR/Cas12a. As a demonstration, DTT was added into NEBuffer r2.1 and NEBuffer r3.1. As expected, both DTT-containing NEBuffer r2.1 and DTT-containing NEBuffer r3.1 significantly enhanced the trans-cleavage efficiency (Fig. 5H). Therefore, the Magigen buffer was selected for the following experiments.

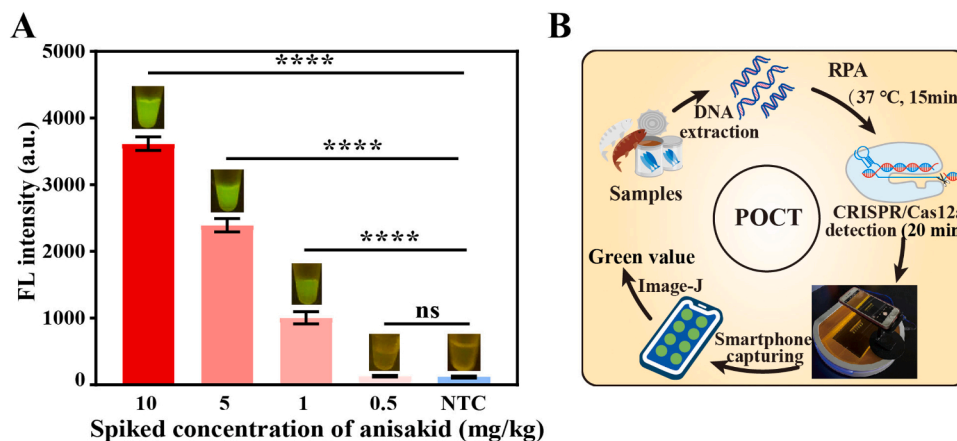
### 3.4. Analytical performance of the biosensing platform

The RPA pre-amplification was integrated with the MoS<sub>2</sub> NSs-CRISPR/Cas12a assay to improve the sensitivity. Then, the biosensing platform was used for detecting a common food-borne parasite (namely *Anisakis* spp.). A series of ten-fold gradient dilutions of *Anisakis* spp. plasmids DNA ( $10^5 - 10^1$  aM) was used as the target DNA for RPA amplification. The amplified products were verified through agarose gel electrophoresis and Sanger sequencing (Fig. S2, S4), indicating the effectiveness of the RPA primers.





**Fig. 6.** Evaluation of MoS<sub>2</sub> NSs-CRISPR/Cas12a assay for detecting *Anisakis* spp. (A) Sensitivity analysis of the proposed assay. (B) The selectivity of the MoS<sub>2</sub> NSs-CRISPR/Cas12a assay. Inset pictures are the visually observing results obtained using a blue light gel imager. Column 1: *Anisakis simplex*; column 2: *Anisakis pegreffii*; column 3: *Anisakis typica*; column 4: *Hysterothylacium aduncum*; column 5: *Clonorchis sinensis*; column 6: *Ligula intestinalis*; column 7: *Trichirurus lepturus* tissue; column 8: ddH<sub>2</sub>O. All nucleic acids of the parasites were at the same concentration. NTC represents no template control.



**Fig. 7.** Applicability of the biosensing assay for detecting *Anisakis* spp. in artificially contaminated fish samples. (A) Detection of fish samples spiked with different proportions of *Anisakis* spp. (B) Schematic diagram of the biosensing strategy applied in the point-of-care testing (POCT) for nucleic acid detection. (C) Minimal instruments needed to perform the proposed biosensing assay. Error bars represent the mean  $\pm$  standard deviation (SD) obtained from three replicates. NTC represents no template control. The unpaired two-tailed t-test was used to analyze the statistical significance. \*\*\*\*,  $P < 0.0001$ ; ns,  $P > 0.05$ .

As illustrated in Fig. 6A, the detection sensitivity was 100 aM, which was 10<sup>7</sup> times higher than that of the detection method without RPA assistance (Fig. S5). The sensitivity was comparable to that of previously reported CRISPR-based methods that combine isothermal amplification techniques for nucleic acid detection [24,26,51,52]. The good sensitivity could be attributed to the highly efficient amplification of RPA, the shearing efficiency of CRISPR/Cas12a and the excellent sensitivity of MoS<sub>2</sub> NSs-based FRET. Subsequently, the selectivity of the constructed biosensor was confirmed by detecting some other fish-borne parasites. Notably, bright green fluorescence signals were observed for *Anisakis* spp., while the group of other fish-borne parasites' nucleic acid and negative control showed no fluorescence signals (Fig. 6B), indicating that the assay was highly selective for *Anisakis* spp. The good selectivity could be attributed to the single-base specificity of CRISPR/Cas12a. Moreover, compared with the ssDNA-FQ reporter, the MoS<sub>2</sub> NSs/ssDNA-FAM reporter shortened the turnaround time by 20 min (Fig. S6).

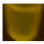
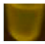
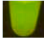
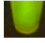


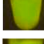
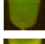
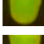
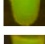
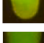



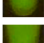
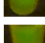
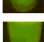

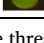

### 3.5. Practicability evaluation

The practicability of the proposed biosensing platform in real

samples was evaluated by spiking fish samples with various concentrations of *A. pegreffii* larvae. The endpoint fluorescence signals were read by a fluorescence microplate reader and a blue light gel imager (Fig. S7). As presented in Fig. 7A, the fluorescence intensity measurement and naked-eye analysis could detect as low as 1 mg/kg of *A. pegreffii* larval spiked in the fish samples. The sensitivity was superior to all the previously described methodologies for *Anisakis* spp. detection (Table S3). Notably, the detection was accomplished within 35 min, which was reduced by at least 50 % compare with that of a real-time PCR method (Table S3). To further minimize the detection time, the RPA and CRISPR/Cas12a system could be performed in one tube. By taking suboptimal PAM strategy, the incompatibility between RPA reaction and CRISPR cleavage reaction could be overcome [53].

In the food monitoring application, simplicity is preferred over sensitivity. Therefore, a miniaturized instrument was used to facilitate POC detection. The workflow was shown in Fig. 7B. In this study, nine replicate analyses of positive samples and corresponding negative controls were performed to validate the feasibility and reliability of this POC detection method. The results of Image J analysis showed that the green values of all negative controls were significantly lower than those of positive controls, demonstrating the feasibility of qualitative analysis

**Table 2**Detection of different fish-derived products artificially contaminated with 10 mg/kg of *A. pegreffii* larvae using the visual method and qPCR assay.

Sample type	No.	Visualization	qPCR*	Sample type	No.	Visualization	qPCR
Controls	Neg		-	Controls	Neg		-
	Pos		+		Pos		+
Baby food	1		+	Smoked	1		+
	2		+		2		+
	3		+		3		+
	4		+		4		+
Canned	1		+	Ready to eat	1		+
	2		+		2		+
	3		+		3		+
	4		+		4		+

“+” means a positive result. “-” means cycle threshold value higher than 35.

\* The qPCR assay was performed according to a previous study [42].

using a portable blue light gel imager (Fig. S8B, C). The results were further validated by detecting the fluorescence intensity. According to the analysis of the green value and fluorescence intensity, the relative standard deviation of nine replicate assays for positive samples was 4.94 % and 5.97 %, respectively (Fig. S8C, E), indicating an acceptable reproducibility of the constructed biosensing platform. Considering the practicality of the visual method, this method was applied to detect fish-derived food samples contaminated with 10 mg/kg of *A. pegreffii* larvae. As shown in Table 2, all the spiked samples produced bright green fluorescence signals, while the negative controls showed no fluorescence. Moreover, the visual results were consistent with those of qPCR tests, confirming that the MoS<sub>2</sub> NSs-CRISPR/Cas12a biosensing platform could be applied in real samples detection. Unlike the PCR-based methods, this assay only needs a heat block and a portable blue light gel imager (Fig. 7C). Therefore, this biosensing platform provides a simple “Yes-or-No” nucleic acid detection answer, holding great potential in POC diagnosis of FBPDs.

#### 4. Conclusion

In summary, a universal CRISPR/Cas12a-based biosensing platform with MoS<sub>2</sub> NSs FRET nanoprobe patterns was constructed for nucleic acid detection. MoS<sub>2</sub> NSs exhibited different adsorption capabilities for different lengths of ssDNA, and the MoS<sub>2</sub> NSs-ssDNA FRET-based system was compatible with the CRISPR/Cas12a system. Under optimal conditions, the detection process could be accomplished within 35 min with attomolar sensitivity for *Anisakis* spp. The proposed biosensing possessed high specificity and satisfying reusability. Additionally, visual observation could be achieved using portable instruments, which is promising for POC applications. Notably, the strategy could be expanded to detect any target nucleic acid due to the codability of gRNA. Overall, this study provides novel perspectives on the viability of a 2D nanomaterials-based reporter in the CRISPR/Cas12a system and has great potential in medical diagnoses.

#### CRedit authorship contribution statement

**Xiuqin Chen:** Conceptualization, Formal analysis, Investigation, Methodology, Writing - original draft, and Writing - review and editing. **Xiaolei Liu:** Formal analysis, Investigation, Methodology, Writing - review & editing. **Yao Yu:** Methodology, Validation, Writing - review & editing. **Haolu Wang:** Investigation and Software. **Chengyao Li:**

Investigation and Software. **Isabelle Vallée:** Investigation and Software. **Mingyuan Liu:** Supervision and Funding acquisition. **Lianjing Zhao:** Conceptualization, Funding acquisition, Writing - review & editing. **Xue Bai:** Supervision, Project administration, and Funding acquisition.

#### Declaration of Competing Interest

The authors declare that they have no known competing financial interests or personal relationships that could have appeared to influence the work reported in this paper.

#### Data Availability

No data was used for the research described in the article.

#### Acknowledgments

This study was supported by the National Key Research and Development Program of China (2021YFC2600202), the National Natural Science Foundation of China (Nos.32230104 and 62101209) and China Postdoctoral Science Foundation Funded Project (No. 2022M710057).

#### Appendix A. Supporting information

Supplementary data associated with this article can be found in the online version at doi:10.1016/j.snb.2023.134493.

#### References

- [1] B. Pang, J. Xu, Y. Liu, H. Peng, W. Feng, Y. Cao, et al., Isothermal amplification and ambient visualization in a single tube for the detection of SARS-CoV-2 using loop-mediated amplification and CRISPR technology, *Anal. Chem.* 92 (2020) 16204–16212.
- [2] L. Wang, X. Wang, Y. Wu, M. Guo, C. Gu, C. Dai, et al., Rapid and ultrasensitive electromechanical detection of ions, biomolecules and SARS-CoV-2 RNA in unamplified samples, *Nat. Biomed. Eng.* 6 (2022) 276–285.
- [3] F. Cui, Y. Yue, Y. Zhang, Z. Zhang, H.S. Zhou, Advancing biosensors with machine learning, *ACS Sens.* 5 (2020) 3346–3364.
- [4] S. Muraru, S. Muraru, F.R. Nitu, M. Ionita, Recent efforts and milestones for simulating nucleic acid FRET experiments through computational methods, *J. Chem. Inf. Model* 62 (2022) 232–239.
- [5] W.R. Algar, N. Hildebrandt, S.S. Vogel, I.L. Medintz, FRET as a biomolecular research tool - understanding its potential while avoiding pitfalls, *Nat. Methods* 16 (2019) 815–829.
- [6] X. Zhang, Y. Hu, X. Yang, Y. Tang, S. Han, A. Kang, et al., Förster resonance energy transfer (FRET)-based biosensors for biological applications, *Biosens. Bioelectron.* 138 (2019), 111314.

- [7] X. Shen, W. Xu, J. Ouyang, N. Na, Fluorescence resonance energy transfer-based nanomaterials for the sensing in biological systems, *Chin. Chem. Lett.* 33 (2022) 4505–4516.
- [8] U. Resch-Genger, M. Grabolle, S. Cavaliere-Jaricot, R. Nitschke, T. Nann, Quantum dots versus organic dyes as fluorescent labels, *Nat. Methods* 5 (2008) 763–775.
- [9] C. Zhu, Z. Zeng, H. Li, F. Li, C. Fan, H. Zhang, Single-layer MoS<sub>2</sub>-based nanopores for homogeneous detection of biomolecules, *J. Am. Chem. Soc.* 135 (2013) 5998–6001.
- [10] G. Oudeng, M. Benz, A.A. Popova, Y. Zhang, C. Yi, P.A. Levkin, et al., Droplet microarray based on nanosensing probe patterns for simultaneous detection of multiple HIV retroviral nucleic acids, *ACS Appl. Mater. Inter.* 12 (2020) 55614–55623.
- [11] Y. Lv, Y. Sun, I. Mahmood Khan, Q. Li, Y. Zhou, L. Yue, et al., Locking-DNA network regulated CRISPR-Cas12a fluorescent aptasensor based on hollow flower-like magnetic MoS<sub>2</sub> microspheres for sensitive detection of sulfadimethoxine, *Chem. Eng. J.* 459 (2023), 141463.
- [12] X. Cheng, Y. Yan, X. Chen, J. Duan, D. Zhang, T. Yang, et al., CRISPR/Cas12a-modulated fluorescence resonance energy transfer with nanomaterials for nucleic acid sensing, *Sens. Actuators B: Chem.* 331 (2021), 129458.
- [13] D.W. Feng, M.X. Ren, Y.F. Miao, Z.R. Liao, T.J. Zhang, S. Chen, et al., Dual selective sensor for exosomes in serum using magnetic imprinted polymer isolation sandwiched with aptamer/graphene oxide based FRET fluorescent ignition, *Biosens. Bioelectron.* 207 (2022), 114112.
- [14] G.W. Xing, N. Li, H.F. Lin, Y.T. Shang, Q.S. Pu, J.M. Lin, Microfluidic biosensor for one-step detection of multiplex foodborne bacteria ssDNA simultaneously by smartphone, *Talanta* 253 (2023), 123980.
- [15] M. Mahani, M. Faghihi-Fard, F. Divsar, M. Torkzadeh-Mahani, F. Khakbaz, Ultrasensitive FRET-based aptasensor for interleukin-6 as a biomarker for COVID-19 progression using nitrogen-doped carbon quantum dots and gold nanoparticles, *Microchim. Acta* 189 (2022) 472.
- [16] M. Dadmehr, M. Mortezaei, B. Korouzhdehi, Dual mode fluorometric and colorimetric detection of matrix metalloproteinase MMP-9 as a cancer biomarker based on AuNPs@gelatin/AuNCs nanocomposite, *Biosens. Bioelectron.* 220 (2023), 114889.
- [17] L.H. Li, M.L. Song, X.Y. Lao, S.Y. Pang, Y. Liu, M.C. Wong, et al., Rapid and ultrasensitive detection of SARS-CoV-2 spike protein based on upconversion luminescence biosensor for COVID-19 point-of-care diagnostics, *Mater. Des.* 223 (2022), 111263.
- [18] J. Wang, L. Sui, J. Huang, L. Miao, Y. Nie, K. Wang, et al., MoS<sub>2</sub>-based nanocomposites for cancer diagnosis and therapy, *Bioact. Mater.* 6 (2021) 4209–4242.
- [19] M. Xiao, T. Man, C. Zhu, H. Pei, J. Shi, L. Li, et al., MoS<sub>2</sub> nanoprobe for microRNA quantification based on duplex-specific nuclease signal amplification, *ACS Appl. Mater. Inter.* 10 (2018) 7852–7858.
- [20] L. Lan, D. Chen, Y. Yao, X. Peng, J. Wu, et al., Phase-dependent fluorescence quenching efficiency of MoS<sub>2</sub> nanosheets and their applications in multiplex target biosensing, *ACS Appl. Mater. Inter.* 49 (2018) 42009–42017.
- [21] Y. Zhao, F. Chen, Q. Li, L. Wang, C. Fan, Isothermal amplification of nucleic acids, *Chem. Rev.* 115 (2015) 12491–12545.
- [22] U. Ganbaatar, C. Liu, NEXT CRISPR: an enhanced CRISPR-based nucleic acid biosensing platform using extended crRNA, *Sens. Actuators B: Chem.* 369 (2022), 132296.
- [23] F. Hu, Y. Liu, S. Zhao, Z. Zhang, X. Li, N. Peng, et al., A one-pot CRISPR/Cas13a-based contamination-free biosensor for low-cost and rapid nucleic acid diagnostics, *Biosens. Bioelectron.* 202 (2022), 113994.
- [24] J.S. Chen, E. Ma, L.B. Harrington, M. Da Costa, X. Tian, J.M. Palefsky, et al., CRISPR-Cas12a target binding unleashes indiscriminate single-stranded DNase activity, *Science* 6387 (2018) 436.
- [25] S. Li, Q. Cheng, J. Liu, X. Nie, G. Zhao, J. Wang, CRISPR-Cas12a has both cis- and trans-cleavage activities on single-stranded DNA, *Cell Res* 28 (2018) 491–493.
- [26] J.S. Gootenberg, O.O. Abudayeh, J.W. Lee, P. Essletzbichler, A.J. Dy, J. Joung, et al., Nucleic acid detection with CRISPR-Cas13a/C2c2, *Science* 6336 (2017) 438–442.
- [27] C. Wu, Z. Chen, C. Li, Y. Hao, Y. Tang, Y. Yuan, et al., CRISPR-Cas12a-empowered electrochemical biosensor for rapid and ultrasensitive detection of SARS-CoV-2 Delta variant, *Nano-Micro Lett.* 14 (2022) 89–100.
- [28] K. Zhang, Z. Fan, B. Yao, Y. Ding, J. Zhao, M. Xie, et al., Exploring the trans-cleavage activity of CRISPR-Cas12a for the development of a Mxene based electrochemiluminescence biosensor for the detection of Siclec-5, *Biosens. Bioelectron.* 178 (2021), 113019.
- [29] S. Lu, F. Li, Q. Chen, J. Wu, J. Duan, X. Lei, et al., Rapid detection of African swine fever virus using Cas12a-based portable paper diagnostics, *Cell Discov.* 6 (2020) 18.
- [30] J. Arizti-Sanz, C.A. Freije, A.C. Stanton, B.A. Petros, C.K. Boehm, S. Siddiqui, et al., Streamlined inactivation, amplification, and Cas13-based detection of SARS-CoV-2, *Nat. Commun.* 11 (2020) 5921.
- [31] P. Ma, Q. Meng, B. Sun, B. Zhao, L. Dang, M. Zhong, et al., McCas12a, a highly sensitive and specific system for COVID-19 detection, *Adv. Sci.* 7 (2020), 2001300.
- [32] T. Li, R. Hu, J. Xia, Z. Xu, D. Chen, J. Xi, et al., G-triplex: A new type of CRISPR-Cas12a reporter enabling highly sensitive nucleic acid detection, *Biosens. Bioelectron.* 187 (2021), 113292.
- [33] H.J. van der Veer, E.A. van Aalen, C.M.S. Michielsen, E.T.L. Hanckmann, J. Deckers, M.M.G.J. van Boren, et al., Glow-in-the-dark infectious disease diagnostics using CRISPR-Cas9-based split luciferase complementation, *ACS Central Sci.* 4 (2023) 657–667.
- [34] Y. Zhang, L. Qian, W. Wei, Y. Wang, B. Wang, P. Lin, et al., Paired design of dCas9 as a systematic platform for the detection of featured nucleic acid sequences in pathogenic strains, *ACS Synth. Biol.* 2 (2017) 211–216.
- [35] Y. Li, S. Li, J. Wang, G. Liu, CRISPR/Cas systems towards next-generation biosensing, *Trends Biotechnol.* 37 (2019) 730–743.
- [36] Y. Tao, K. Yi, H. Wang, K. Li, M. Li, Metal nanoclusters combined with CRISPR-Cas12a for hepatitis B virus DNA detection, *Sens. Actuators B: Chem.* 361 (2022), 131711.
- [37] S.A.E. Marras, F.R. Kramer, S. Tyagi, Efficiencies of fluorescence resonance energy transfer and contact-mediated quenching in oligonucleotide probes, *Nucleic Acids Res.* 30 (2002), e122.
- [38] X. Mu, J. Li, S. Xiao, J. Xu, Y. Huang, S. Zhao, et al., Peroxidase-mimicking DNA-Ag/Pt nanoclusters mediated visual biosensor for CEA detection based on rolling circle amplification and CRISPR/Cas 12a, *Sens. Actuators B: Chem.* 375 (2023), 132870.
- [39] J. Li, J. Zhu, K. Xu, Fluorescent metal nanoclusters: from synthesis to applications, *Trends Anal. Chem.* 58 (2014) 90–98.
- [40] L. Zhang, E. Wang, Metal nanoclusters: new fluorescent probes for sensors and bioimaging, *Nano Today* 9 (2014) 132–157.
- [41] D. Qi, C. Wang, Y. Gao, H. Li, Y. Wu, Heteroatom doping and supramolecular assembly promoted copper nanoclusters to be a stable & high fluorescence sensor for trace amounts of ATP determination, *Sens. Actuators B: Chem.* 358 (2022), 131469.
- [42] X. Chen, L. Zhao, J. Wang, H. Wang, Y. Qiu, Z. Dong, et al., Rapid visual detection of anisakid nematodes using recombinase polymerase amplification and SYBR Green I, *Front. Microbiol.* 13 (2022), 1026129.
- [43] L. Zhao, M. Cheng, G. Liu, H. Lu, Y. Gao, X. Yan, et al., A fluorescent biosensor based on molybdenum disulfide nanosheets and protein aptamer for sensitive detection of carcinoembryonic antigen, *Sens. Actuators B: Chem.* 273 (2018) 185–190.
- [44] F. Hu, Y.F. Liu, S.H. Zhao, Z.M. Zhang, X.C. Li, N.C. Peng, et al., A one-pot CRISPR/Cas13a-based contamination-free biosensor for low-cost and rapid nucleic acid diagnostics, *Biosens. Bioelectron.* 202 (2022), 113994.
- [45] Y. Wu, Y. Dong, Y. Shi, H. Yang, J. Zhang, M.R. Khan, et al., CRISPR-Cas12-based rapid authentication of halal food, *J. Agr. Food Chem.* 35 (2021) 10321–10328.
- [46] H. Lv, J. Wang, J. Zhang, Y. Chen, L. Yin, D. Jin, et al., Definition of CRISPR Cas12a trans-cleavage units to facilitate CRISPR diagnostics, *Front. Microbiol.* 12 (2021), 766464.
- [47] J.D.D. Habimana, O. Mukama, G. Chen, M. Chen, O.B. Amisah, L. Wang, et al., Harnessing enhanced CRISPR/Cas12a trans-cleavage activity with extended reporters and reductants for early diagnosis of *Helicobacter pylori*, the causative agent of peptic ulcers and stomach cancer, *Biosens. Bioelectron.* 222 (2023), 114939.
- [48] L. Zhao, D. Kong, Z. Wu, G. Liu, Y. Gao, X. Yan, et al., Interface interaction of MoS<sub>2</sub> nanosheets with DNA based aptamer biosensor for carbohydrate antigen 15-3 detection, *Microchem. J.* 155 (2020), 104675.
- [49] X. Ding, X. Kong, Y. Chen, C. Zhang, Y. Hua, X. Li, Selective extraction and antioxidant properties of thiol-containing peptides in soy glycinine hydrolysates, *Molecules* 23 (2018) 1909.
- [50] H. Ding, C. Liang, K. Sun, H. Wang, J.K. Hiltunen, Z. Chen, et al., Dithiothreitol-capped fluorescent gold nanoclusters: an efficient probe for detection of copper (II) ions in aqueous solution, *Biosens. Bioelectron.* 59 (2014) 216–220.
- [51] X. Luo, Y. Xue, E. Ju, Y. Tao, M. Li, L. Zhou, et al., Digital CRISPR/Cas12b-based platform enabled absolute quantification of viral RNA, *Anal. Chim. Acta* 1192 (2022), 339336.
- [52] Y. Zhang, M. Chen, C. Liu, J. Chen, X. Luo, Y. Xue, et al., Sensitive and rapid on-site detection of SARS-CoV-2 using a gold nanoparticle-based high-throughput platform coupled with CRISPR/Cas12-assisted RT-LAMP, *Sens. Actuators B: Chem.* 345 (2021), 130411.
- [53] S. Lu, X. Tong, Y. Han, K. Zhang, Y. Zhang, Q. Chen, et al., Fast and sensitive detection of SARS-CoV-2 RNA using suboptimal protospacer adjacent motifs for Cas12a, *Nat. Biomed. Eng.* 6 (2022) 286–297.

**Xiuqin Chen** received her MS degree in 2014 from South China Agricultural University, China. She currently works at Fujian Academy of Agricultural Science and is currently a PhD candidate at Jilin University, China. Her current research focus on the development of CRISPR/Cas-based molecular diagnosis and rapid detection of food-borne parasites.

**Xiaolei Liu** received his PhD in 2012 from Jilin University, China. He is currently a professor at Jilin University, board member of International Commission of Trichinellosis (ICT) and member of OIE Collaborating Centre for Food-Borne Parasites from the Asian-Pacific Region. His major researches focus on Trichinellosis and Clonorchiasis.

**Yao Yu** received her MS degree in 2022 from Jilin University, China. Currently, she is currently a PhD student at Jilin University, China. Her current research interests are the detection, prevention and control of food-borne parasites and the analysis of food safety of animal origin.

**Haolu Wang** received her BS degree in 2020 from Northwest Sci-Tech University of Agriculture and Forestry, China. She is a student studying for her MS's degree at the College of Veterinary Medicine, Jilin University, China. Her research interests mainly focus on the development of CRISPR/Cas-based molecular diagnosis and rapid detection of food-borne parasites.

**Chengyao Li** is currently a PhD candidate at Jilin University. Her research focuses on the interaction between trichinella spiralis and hosts.

**Isabelle Vallée** received her PhD in 1996. She is currently the head of the Parasites and Fungi Research Department at the Animal Health Laboratory of the French Agency for Food Safety, Environment and Occupational Health (ANSES) and head of the WOAHE European Collaborating Centre for Foodborne Animal and Human Parasites. Her research interests mainly focus on the important foodborne parasites.

**Mingyuan Liu** received his PhD in 2004 from University of Paris XII. He is currently a professor at Jilin University, board member of International Commission of Trichinellosis (ICT) and contact point of OIE Collaborating Centre for Food-Borne Parasites from the Asian-Pacific Region. His major researches focus on food-borne zoonosis including Trichinellosis and Clonorchiasis with more than 20 national and international projects.

**Lianjing Zhao** received her M.S. degree from College of Life Science (2013) and PhD degree from College of Electronic Science and Engineering (2020), Jilin University, China. Subsequently she was appointed the lecturer in Jilin University in 2021. Her research interests mainly focus on the development of the functional nanomaterials and their applications in biosensor and chemical sensor.

**Xue Bai** received her PhD in 2011 from Jilin University, China. She is currently a professor at Jilin University. In 2016, as member joined in OIE Collaborating Center for Food-borne Parasites in the Asian-Pacific Region and International Committee on Trichinellosis (ICT). Her major researches focus on regulation and evasion of host immune response by parasitic helminths and diagnosis of foodborne parasite disease.